Environ Monit Assess (2022) 194: 289
https://doi.org/10.1007/s10661-022-09951-4

Exploring the causes for co-pollution of O_3 and $PM_{2.5}$ in summer over North China

Shengju Ou · Wei Wei · Bin Cai · Shiyin Yao · Kai Wang · Shuiyuan Cheng

Received: 18 September 2021 / Accepted: 12 March 2022 / Published online: 21 March 2022

Abstract Co-pollution of surface O_3 and $PM_{2.5}$ has become the most predominant type of air pollutions in Beijing-Tianjin-Hebei region in the hot season since 2017, particularly in May–July. Analysis based on observational data showed that co-pollution was always accompanied by high temperature, moderate relative humidity, extremely high SO_2, and higher NO_2. We also found that the meteorology and precursor dependence of O_3 was similar between co-pollution and O_3- single pollution. While $PM_{2.5}$ in co-pollution was more related to temperature, relative humidity, and precursors, that in $PM_{2.5}$-singe pollution were more related to small winds. These results indicate that co-pollution seemed to be more affected by atmospheric chemistry. According to the $PM_{2.5}$ components, secondary inorganic aerosols (SIA) composed 44.3–48.7% of $PM_{2.5}$ in co-pollution, while those accounting for 42.1–46.5% and 41.2–44.3%, respectively, in O_3- and $PM_{2.5}$-single pollution, which further confirmed the relatively stronger atmospheric chemistry processes in co-pollution. And the high proportion of SIA in co-pollution was mainly attributed to SO_4^{2-}, which was observed to rapidly boom in non-refractory submicron aerosol (NR-PM_1) on the condition of high level of O_3 at daytime. Additionally, we further explored the interactions of O_3 and $PM_{2.5}$ in co-pollution. It was found that most (~61.9%) co-pollution episodes were initiated by high O_3 at daytime; while for other episodes, high $PM_{2.5}$ firstly occurred under the more stable meteorological conditions, and then accumulation of precursors further induced high O_3. A higher SIA concentration was observed in O_3-initiated co-pollution, indicating that the atmospheric oxidation in co-pollution caused by chemical processes was stronger than that by physical processes, which was further approved by the higher values of SOR and NOR in O_3-initiated co-pollution. This observational study revealed that controlling O_3 and precursor SO_2 is the key to abating co-pollution in the hot season.

Keywords Co-pollution · Surface O_3 and $PM_{2.5}$ · Meteorology · Precursors · High level of oxidation products

Highlights

- Co-pollution means daily maximum 8-h average $O_3 > 160$ μg/m^3 and daily mean $PM_{2.5} > 35$ μg/m^3.
- Co-pollution prevailed in May–July, characterized by high level of oxidative products.
- Approximately 61.9% of co-pollution episodes were initiated by O_3 pollution.
- High level of SO_2 was the key for initiation of $PM_{2.5}$ booming by O_3.
- Rapid oxidation of NO_x at night was the key for initiation of $PM_{2.5}$ booming by O_3.

S. Ou · W. Wei (✉) · B. Cai · S. Yao · K. Wang · S. Cheng
Key Laboratory of Beijing on Regional Air Pollution Control, Beijing University of Technology, 100124 Beijing, China
e-mail: weiwei@bjut.edu.cn

Introduction

In recent years, the emissions of major air pollutants, such as sulfur dioxide (SO_2), nitrogen oxides (NO_x),

carbon monoxide (CO), and primary $PM_{2.5}$, have significantly decreased in Beijing-Tianjin-Hebei (BTH) region due to the implementation of the China's Clean Air Action Plans and thus resulted in $PM_{2.5}$ improvement (Zhang et al., 2019a, b). However, $PM_{2.5}$ concentration has not yet reached the standard that is recommended by the World Health Organization despite in the hot season with a low level of $PM_{2.5}$. Additionally, the surface O_3 pollution has been worsening in this region in recent years (Li et al., 2019), which has become an important pollutant affecting the air quality following $PM_{2.5}$, thus bringing about the frequent occurrence of co-pollution of O_3 and $PM_{2.5}$. Both O_3 and $PM_{2.5}$ cause adverse effects on health (Zhang et al., 2017), air quality (Angelevska et al., 2021; Fenech et al., 2019), visibility (Xu et al., 2020), and climate change (Yang et al., 2020). Therefore, it is of critical importance to explore the causes of surface O_3 and $PM_{2.5}$ pollution for addressing the issue of air pollution.

A large body of studies were conducted on either summer O_3 or winter $PM_{2.5}$ to understand the pollution characteristics and source apportionment (Zha et al., 2021; Cheng et al., 2021; Shu et al., 2020). It is found that high level of gaseous precursors was the prerequisites leading to the occurrence of O_3 and $PM_{2.5}$ pollution (Chen et al., 2020; Hughes et al., 2021; Kuerban et al., 2020). And the O_3 pollution in summer was always accompanied with high temperature and low relative humidity (Ma et al., 2021b; Yu et al., 2019), while the $PM_{2.5}$ pollution frequently occurred under the stagnant weather conditions (i.e., high relative humidity and small winds) (Ma et al., 2021b; Wang et al., 2021). Besides, the occurrence of O_3 pollution was the joint effects of local photochemistry and regional transport, and the latter was usually dominated in most pollution episodes (Gong et al., 2020), because the O_3 pollution is a regional issue. By contrast, the $PM_{2.5}$ pollution was more a sensitive response to the local emission. Existing studies were mostly focused on O_3 or $PM_{2.5}$ pollution. However, study on the co-pollution of these two pollutants and the interaction between them is limited.

$PM_{2.5}$ and O_3 can affect each other in the atmosphere. Theoretically, as airborne aerosols, $PM_{2.5}$ can weaken the photolysis processes through absorbing or scattering solar radiation and reduce the precursors through being consumed by aerosol chemistry, which would be adverse to photochemical O_3 production (Liu & Wang, 2020a, b; Li et al., 2019). Thus, surface O_3 is expected to increase (decrease) with the noticeable decline (rise) of $PM_{2.5}$ concentrations. Shao et al. (2021) reported that O_3 formation increased by 37% in 2006–2016 due to $PM_{2.5}$ dropping in Beijing. Ma et al. (2021a, b) documented that aerosol radiative forcing accounted for ~23% of the total change in surface O_3 over North China Plain in summer of 2013–2019. Previous study has revealed that the atmospheric oxidation capacity is the essential driving force of atmospheric chemistry in forming complex air pollution, which determines the removal rate of trace gases and also the production rates of secondary pollutants (Lu et al., 2019). O_3 as an important atmospheric oxidant, can enhance the atmospheric oxidation capacity and thereby promote the conversion of gaseous precursors (i.e., SO_2, NO_2, and NH_3, etc.) into secondary particles (i.e., SO_4^{2-}, NO_3^- and NH_4^+, etc.), and eventually induce $PM_{2.5}$ pollution (Zhao et al., 2020). Numerous studies have demonstrated that more than half of the components in $PM_{2.5}$ are secondary particles in China (Liu et al., 2021; Wang et al., 2020), indicating the atmospheric oxidation capacity plays a crucial role in the air pollution of China. Besides, an increase in O_3 is usually accompanied with the rise in OH radicals (the most chemically active component in atmosphere), and thereby further enhance the atmospheric oxidation capacity. This is because that the $O(^1D)$ generated from O_3 photolysis reacting with H_2O is another important source of OH (Shao et al., 2004). Overall, O_3 pollution will further enhance $PM_{2.5}$ pollution, and $PM_{2.5}$ pollution will enhance or inhibit O_3 pollution to some extent.

Therefore, to explore the characteristics and causes of co-pollution based on surface O_3 and $PM_{2.5}$ in the hot season in BTH, we researched the co-pollution of O_3 and $PM_{2.5}$ according to the observations in 2015–2019. We aimed to (a) obtain the variation trends of co-pollution under the conditions of continuous declined $PM_{2.5}$ and aggravated O_3, (b) investigate what the meteorological and chemical conditions when co-pollution occurred were; (c) figure out how the atmospheric oxidation capacity changed in co-pollution by analyzing the variations of secondary inorganic aerosols and its oxidation ratio; and (d) explore the interactions of O_3 and $PM_{2.5}$ in co-pollution. Overall, our research results provide a better understanding of co-pollution from the perspective of observations.

Materials and methods

Conception of co-pollution

As mentioned previously, $PM_{2.5}$ and O_3 can affect each other in the atmosphere. The observational data showed that the summer daily mean $PM_{2.5}$ concentration in China in recent years is lower than 75 μg/m^3 but far higher than 35 μg/m^3 that is recommended by the World Health Organization guidelines. In addition, considering the national ambient air quality standards (NAAQS) Grade II (35 μg/m^3) of annual mean $PM_{2.5}$ concentration, a certain day in which the MDA8 O_3 concentration being above 160 μg/m^3 or/and the daily mean $PM_{2.5}$ concentration above 35 μg/m^3 was recognized as a polluted day in this study. The study period in May–September of 2015–2019 was divided into four groups based on the O_3 and $PM_{2.5}$ concentrations above-mentioned: O_3-single pollution (MDA8 $O_3 > 160$ μg/m^3 and $PM_{2.5} < 35$ μg/m^3), $PM_{2.5}$-single pollution (MDA8 $O_3 < 160$ μg/m^3 and $PM_{2.5} > 35$ μg/m^3), co-pollution (MDA8 $O_3 > 160$ μg/m^3 and $PM_{2.5} > 35$ μg/m^3), and non-pollution (MDA8 $O_3 < 160$ μg/m^3 and $PM_{2.5} < 35$ μg/m^3).

Pollutants and meteorological data

The hourly mass concentrations of pollutants, including surface O_3, $PM_{2.5}$, NO_2, SO_2, and CO in May–September of 2015–2019, were taken from the China National Environmental Monitoring Centre website (CNEMC, http://www.cnemc.cn/). The surface meteorological parameters at 1-h intervals, including wind speed (WS), wind direction, temperature (T), and relative humidity (RH), were obtained from the China Meteorological Administration observation network (http://data.cma.cn/).

Measurement of main compositions in $PM_{2.5}$

Beijing-Tianjin-Hebei region is located at the northern of the North China Plain, surrounded by the Yanshan Mountains to the north, the Taihang Mountains to the west, the Bohai Bay to the east, and plains to the south. It encompasses two municipalities (Beijing and Tianjin) and one province (Hebei), as shown in Fig. 1. This region is one of the most economically vibrant regions in China. A detailed description of this region can be found in a previous study (Guo et al., 2020). In this study, three cities with obviously different emission structures were chosen to explore the characteristics in co-pollution. Beijing (BJ) is an international and post-industrialization megacity that emits less air pollutant due to less industries compared with other two cities. Tangshan (TS) is an industrial city, resulting in emitting many more air pollutants. Shijiazhuang (SJZ) is the capital city of Hebei province, which is dominated by light industry; thus the emissions of air pollutant level are between BJ and TS.

Integrated $PM_{2.5}$ samples were collected on a day-by-day schedule in BJ, SJZ, and TS in summers (July) from 2015 to 2019. The three sampling sites were surrounded by offices, residential areas, and traffic, and all were placed on the rooftop of a certain office building (approximately 20 m from the ground level), which can be a representative of the urban environment. $PM_{2.5}$ samples were collected on the 90 mm cellulose filters (Whatman Inc. Maidstone, UK) lasting for 24 h per day (from 10:00 am to 9:00 am in the sample collection day) at a volumetric flow rate of 100 L/min. Finally, filters were collected to examine $PM_{2.5}$ and its chemical compositions, comprising of water-soluble ions and carbonaceous materials. The filters were pre- and post-weighed using an electronic microbalance with an accuracy of 0.01 mg (Sartorius TB-215D, Germany) in a super-clean room with the constant temperature (20 ± 5 °C) and humidity (40 ± 2%) for 48 h. After weighing, the samples were stored in a refrigerator at −18 °C.

For analyzing of water-soluble ions concentrations, a quarter of each sample was extracted ultrasonically using 10-mL distilled-deionized water and oscillated for 40 min in a supersonic cleaner. Sulfates (SO_4^{2-}), nitrates (NO_3^-), and ammonium salts (NH_4^+) were measured by ion chromatography (Metrohm 861 Advanced Compact IC, Switzerland). Carbonaceous concentrations, including organic carbon (OC) and elemental carbon (EC), were measured using a thermal/optical carbon analyzer (DRI Model 2001A, Desert Research Institute of the United States). All the above-mentioned operations were conducted in accordance with quality control standards to avoid any possible contamination in the membrane samples. More detailed analytical procedures for water-soluble ions and carbonaceous aerosols as well as quality control can be found in a previous study (Wang et al., 2015).

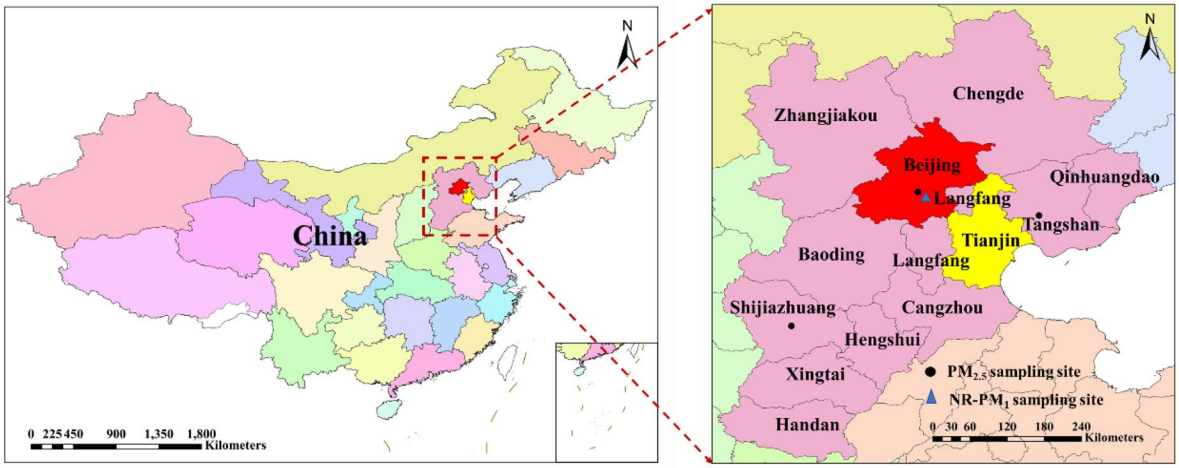

Fig. 1 Location of the BTH region and the sampling sites ($PM_{2.5}$ sampling site located in Beijing, Shijiazhuang, and Tangshan; NR-PM_1 sampling located site in Beijing)

NR-PM_1 components measurement at 1-h resolution

Previous study reported that secondary inorganic aerosols (SIA, including SO_4^{2-}, NO_3^-, NH_4^+) are mostly gathered in particles with an aerodynamic diameter of less than 1 μm (Zhang et al., 2018). Thus, based on the daily $PM_{2.5}$ results, non-refractory submicron aerosol (NR-PM_1) components at a higher time resolution (at 1–h) were applied to explore the characteristics of secondary particles in co-pollution. Concentrations of NR-PM_1 components, including SO_4^{2-}, NO_3^-, and organics (Org) in the hot season from 2017 to 2019, were measured by an Aerodyne Aerosol Chemical Speciation Monitor (ACSM) at the Beijing University of Technology (BJUT). The BJUT sampling site (39.88° N, 116.49° E) was located between the southeastern third and fourth ring roads in Beijing, which is surrounded by traffic, residential, and business districts and does not have a stationary pollution source in the vicinity. The ACSM data were analyzed for mass concentration and composition using the ACSM standard data analysis software written in Igor Pro. The output data was at a 15-min time resolution, which was further computed into 1-h resolution to match the precursor concentrations. More detailed descriptions of this instrument and data analysis have been provided in a previous study (Han et al., 2019).

Results and discussion

Occurrence frequency and intensity of co-pollution

According to the definition of co-pollution of O_3 and $PM_{2.5}$, its occurrence frequency in 13 cities of BTH was firstly calculated in the hot season over 2015–2019, as well as that of O_3-single pollution, $PM_{2.5}$-single pollution, and non-pollution. Figure 2 illustrates the proportions of these pollution types in various years and months at regional and local scales. Generally, co-pollution accounted for 24.3–35.6% during 2015–2019 on 13-city average and became the most predominant type since 2017 (Fig. 2a). This is because that although $PM_{2.5}$ pollution has been alleviated over the last few years due to the implementation of the China's Clean Air Action Plans, $PM_{2.5}$ concentration has not yet reached the standard that is recommended by World Health Organization guidelines; in addition, the O_3 pollution have been worsening in recent years. Therefore, the co-pollution has become more and more predominant in the hot season. Regarding the monthly variations (Fig. 2b), co-pollution prevailed in May–July, whose proportion reached up to 35.7–44.6% and greatly higher than that in August–September (18.7–21.0%). One most possible reason is that the temperature in May–July is relatively higher than that in August–September, thus

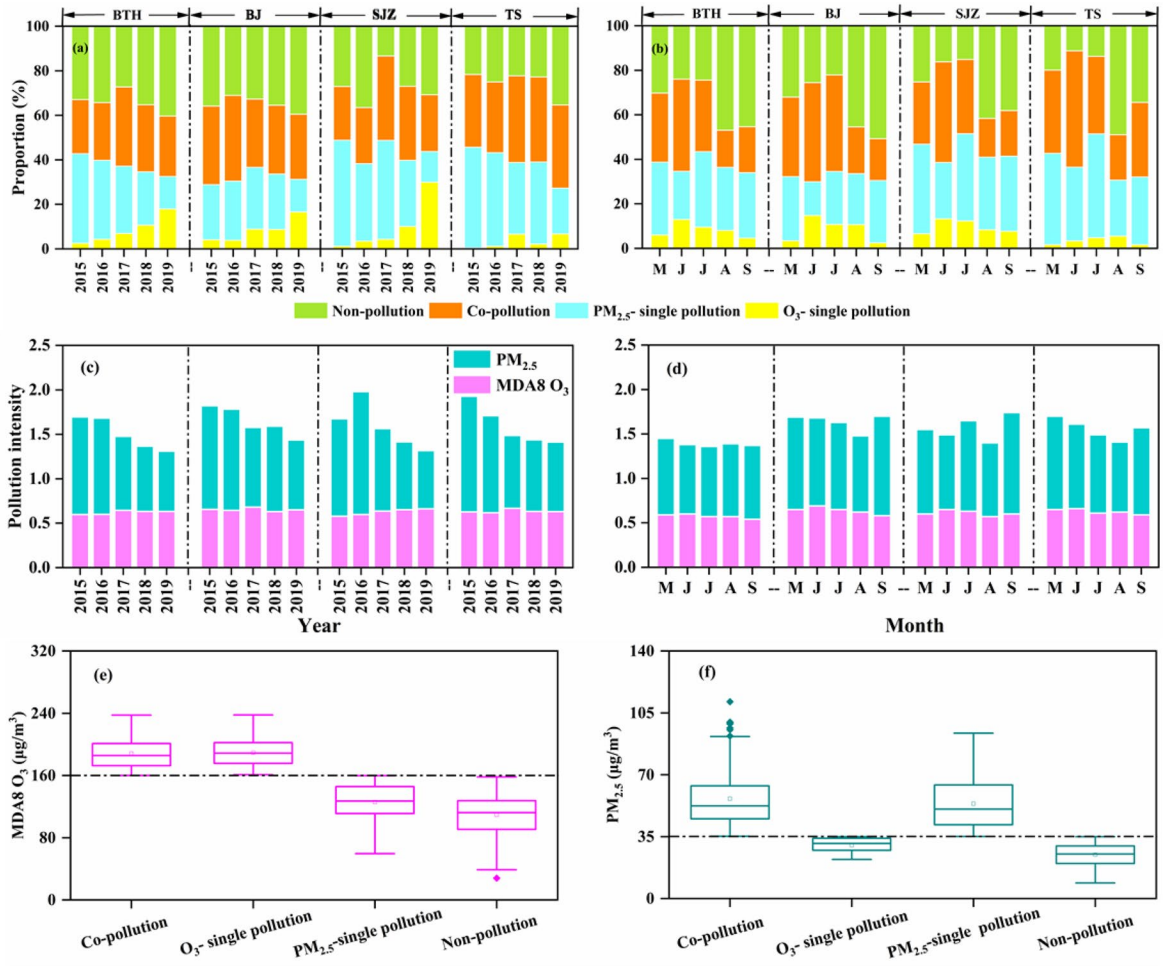

Fig. 2 Occurrence frequency (**a**, **b**) and intensity (**c**, **d**), concentrations of MDA8 O_3 and $PM_{2.5}$ (**e**, **f**) in co-pollution during the study period in BTH

leading to the more enhanced atmospheric oxidation capacity due to more occurrence of O_3 pollution and further inducing the co-pollution. Additionally, better atmospheric diffusion conditions are usually found in August–September than those in May–July, such as higher mixing layer height, more precipitations, and more windy days, which are conducive to the diffusion of pollutants. The corresponding interannual and monthly changes also presented a good similarity in BJ (international metropolis), SJZ (province capital city), and TS (industrial city), which implied the regional characteristics of co-pollution of O_3 and $PM_{2.5}$ in hot season over BTH.

Then, we quantified the pollution intensity (PI) of co-pollution according to Eq. (1), in which O_3 and $PM_{2.5}$ pollutants were equally considered.

$$PI = \frac{C_{\text{MDA8 O}_3}}{160} \times 0.5 + \frac{C_{\text{daily PM}_{2.5}}}{35} \times 0.5 \quad (1)$$

Figure 2c shows that PI values of co-pollution presented a discernible decreasing trend, from 1.69 in 2015 to 1.31 in 2019 on 13-city average, which was mostly attributed to the greatly evident decline in $PM_{2.5}$. To PI values, the contribution of O_3 largely increased from 35.3% in 2015 to 48.2% in 2019; conversely, the corresponding contribution of $PM_{2.5}$

gradually reduced in this period. These results indicated that combined roles of O_3 and $PM_{2.5}$ in air quality over BTH became more and more significant, further suggesting that more attention should be paid to co-pollution in the future. However, the PI values and their contributors varied little in different months (Fig. 2d), which might be balanced by the decreased $PM_{2.5}$ and increased O_3 occurred in various months. During the whole study period in BTH, the mean MDA8 O_3 concentration in co-pollution type was close to that in O_3-single pollution type but higher by 49.5% than that in $PM_{2.5}$-single pollution type (Fig. 2e); while the mean of daily $PM_{2.5}$ concentration in co-pollution type was higher than that in O_3- and $PM_{2.5}$-single pollution types, respectively, by 87.7% and 5.2% (Fig. 2f). It means that the more serious harm of co-pollution type compared to two single pollution types because of the integrated effects of $PM_{2.5}$ and O_3.

Characteristics of meteorology and precursors in co-pollution

Then, we further investigated the meteorological and chemical conditions of co-pollution in BJ, SJZ, and SJZ three cities. The average diurnal patterns of surface temperature (T), relative humidity (RH), and wind speed (WS) as well as precursors of SO_2, NO_2, and CO in May–September of 2015–2019 were summarized in Fig. 3. It demonstrated that co-pollution type was always accompanied by high T (daily mean of 25.8–28.2 ℃), moderate RH (daily mean of 55.4–63.5%), extremely high SO_2 (daily mean of 5.9–31.1 μg/m^3), and higher NO_2 (daily mean of 36.1–49.8 μg/m^3). During the co-pollution, the high T can facilitate O_3 formation through directly controlling temperature-dependent photochemical reactions or indirectly promoting precursors emitting from anthropogenic and biogenic sources based on temperature (Liu & Wang, 2020b; Porter & Heald, 2019); in addition, under the conditions of high T and high gas precursors, the moderate RH can be conductive to the formation of secondary particles (i.e., SO_4^{2-}, NO_3^-, etc.), thus leading to the increase in $PM_{2.5}$ concentration. Unexpectedly, small winds were not found in co-pollution, in which the wind speed was comparable among all pollution types. Compared with co-pollution, O_3-single pollution had the lower RH (lower by ~11.7% except TS), SO_2 (lower by ~27.5%), and CO (lower by ~30.0%) but presenting the similar levels of T and NO_2, while $PM_{2.5}$-single pollution had the lower T (lower by ~11.4%), higher RH (higher by 14.9%), and lower SO_2 (lower by 27.1% except TS) but the similar levels of NO_2 and CO. It can be seen high T and abundant NO_2 was the essential condition of O_3-single pollution and co-pollution; and then the participation of high level of SO_2 facilitated the $PM_{2.5}$ increase through aerosol chemistry, thus eventually inducing the co-pollution of O_3 and $PM_{2.5}$. Additionally, CO concentrations in co-pollution were comparable to those in $PM_{2.5}$-single pollution but far higher than those in O_3-single pollution and non-pollution. These results also implied the important role of physical accumulation in co-pollution type, as well as in $PM_{2.5}$-single pollution type. This is as a result of a fact that CO is not active photochemical, whose chemical life can last for several months; it can be seen as an inert pollution tracer in a short period and is mainly influenced by meteorological factors (Zhang et al., 2015). Therefore, the high level of CO means that poor atmospheric diffusion conditions occurred.

In addition, we applied multiple linear regression (MLR) method based on the Statistical Product and Service Solutions (SPSS) to further quantify the relationship among co-pollution and meteorological parameters and precursors during June, in which the co-pollution most frequently occurred compared with other months of the hot season (Fig. 2b). In this study, the values of confidence (i.e., Sig.) were all far lower than 0.05, indicating that the linear regression equations were meaningful. Besides, the variance inflation factor (VIF) was in the range of 1.1–4.5 and were lower than 10, demonstrating no collinearity among all variables (Fox & Monette, 1992). Table 1 summarizes the linear regression equation of hourly O_3 or $PM_{2.5}$ concentrations with meteorological parameters ([T], [RH], and [WS]) and precursors ([SO_2], [NO_2], and [CO]) under different pollution types.

As for O_3, the regression coefficients of all factors (except for WS) showed a comparable level in co-pollution (Co_O_3) and O_3-single pollution (Single_O_3), further indicating that the causes of O_3 formation in the two pollution types were similar, which was consistent with the results observed in Fig. 3. The coefficient value of WS in Co_O_3 was significantly higher than that in Single_O_3, which could imply that the effect of transport on O_3 in co-pollution could be bigger than that in O_3-single

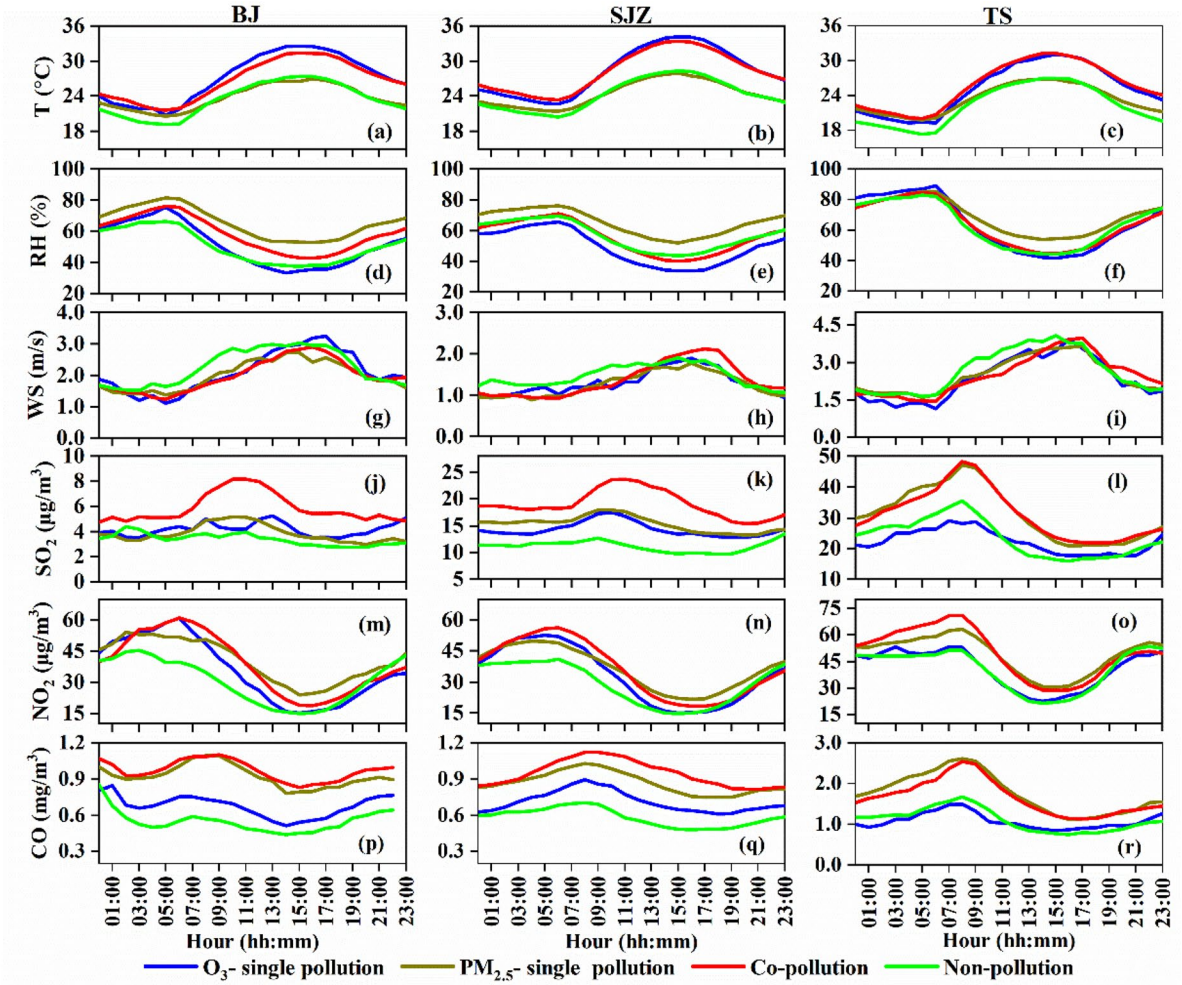

Fig. 3 Diurnal variations of meteorological parameters and precursors in co-pollution during the study period in BJ, SJZ, and TS

pollution. Regarding $PM_{2.5}$, the regression coefficients presented significant differences between co-pollution (Co_$PM_{2.5}$) and $PM_{2.5}$-single pollution (Single_$PM_{2.5}$), particularly the coefficients of T and RH being higher in co-pollution, which suggested that $PM_{2.5}$ in co-pollution was more dependent on high T and RH than that in $PM_{2.5}$-single pollution. Besides, the regression coefficient of SO_2 was negative and more significant in co-pollution, which highlighted that the chemical formation of $PM_{2.5}$ played a dominant role in co-pollution, while the regression coefficient of WS was negative and more pronounced in $PM_{2.5}$-single pollution, indicating that the small wind was obvious and the

Table 1 Linear regression equation of O_3 or $PM_{2.5}$ under different pollution types

Index	Linear regression equation
O_3	Co_ $O_3 = 0.615[T] + 0.032[RH] + 0.170[WS] + 0.036[SO_2] - 0.361[NO_2] + 0.020[CO]$
	Single_ $O_3 = 0.744[T] + 0.126[RH] + 0.086[WS] - 0.083[SO_2] - 0.331[NO_2] + 0.052[CO]$
$PM_{2.5}$	Co_ $PM_{25} = 0.544[T] + 0.537[RH] - 0.002[WS] - 0.181[SO_2] + 0.246[NO_2] + 0.367[CO]$
	Single_ $PM_{25} = 0.198[T] + 0.337[RH] - 0.211[WS] - 0.019[SO_2] + 0.218\ [NO_2] + 0.294[CO]$

physical accumulation might be the driving force in $PM_{2.5}$-single pollution. In general, quantitative relationships among meteorological parameters and precursors would be helpful for better understanding the occurrence of co-pollution.

Characteristics of high level of oxidation products in co-pollution

SIA of daily $PM_{2.5}$ in July

Both ozone and secondary $PM_{2.5}$ are deeply related to atmospheric oxidation reactions. The major secondary inorganic aerosols (SIA) include SO_4^{2-}, NO_3^-, and NH_4^+, in which SO_4^{2-} and NO_3^- are directly generated from the oxidations of SO_2 and NO_x and NH_4^+ is converted from NH_3 to neutralize the acid aerosols. Thus, the bigger the content of SIA in particles is, the more aged and oxidized the atmosphere is. According to the $PM_{2.5}$ measurements in BJ, SJZ, and TS, the average proportions of SIA and other components in July were obtained and summarized in Fig. 4. It can be seen the total proportion of three inorganic salts was the highest in co-pollution type and accounted for 44.3–48.7% of $PM_{2.5}$; $PM_{2.5}$-single pollution (with proportion of 42.1–46.5%) and O_3-single pollution (with proportion of 41.2–44.3%) followed, while, the corresponding proportion in non-pollution was the lowest (with proportion of 35.7–40.6%). These results further illustrated more formation of secondary particles in co-pollution under the condition of a strong oxidative air condition with high level of O_3 concentrations.

The increase of SIA proportion in co-pollution type compared with $PM_{2.5}$-single pollution type was mainly derived from SO_4^{2-} (increasing by 12.0–18.0%) and NH_4^+ (increasing by 4.3–7.7%), but negatively affected by NO_3^- (decreasing by 0.2–3.9%), which was associated with the fact that NO_3^- generated by photochemical reactions could not overcome or offset the effects of NO_3^- volatilization induced by the high temperature, particularly after noon (Zhang et al., 2018). While the increase of SIA proportion in co-pollution type compared with O_3- single pollution type resulted from the enhancement of SO_4^{2-}, NO_3^-, and NH_4^+, with contribution of 15.3–17.1%, 13.1–16.0%, and 11.5–12.9%, respectively, in general, the contribution of SO_4^{2-} to $PM_{2.5}$ played a more predominant role than NO_3^- and NH_4^+, particularly in the co-pollution type. This

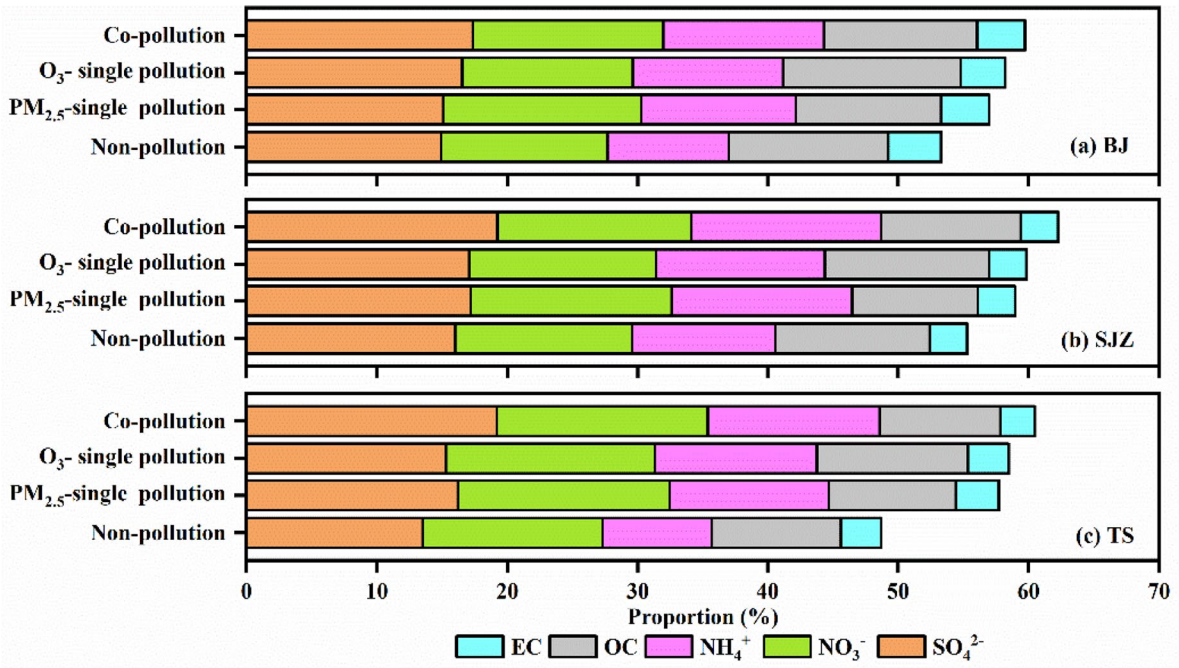

Fig. 4 Variation of main $PM_{2.5}$ compositions in co-pollution over July of 2015–2019 in BJ, SJZ, and TS

could be explained by the extremely high level of SO_2 in co-pollution facilitating the evident increase in $PM_{2.5}$ through aerosol chemistry (see in Fig. 3). In addition, the ratios of OC/EC varied among different pollution types, following the order of O_3-single pollution $(4.03 \pm 0.37) >$ co-pollution $(3.47 \pm 0.27) > PM_{2.5}$-single pollution (3.12 ± 0.22), demonstrating that the atmosphere oxidation was relatively more intense in co-pollution and thus strengthen the production of oxidation products (i.e., SIA and OC) and finally led to $PM_{2.5}$ increase.

SIA of hourly NR-PM_1 in May–September

In this study, ACSM analyzer was applied in BJ to measure the compositions of particle with an aerodynamic diameter of less than 1 μm (NR-PM_1) at the time resolution of 1-h. The temporal characteristics of the secondary aerosols in co-pollution are further explored according the NR-PM_1 and its components, as shown in Fig. 5. NR-PM_1 mass concentration in co-pollution during May–September of 2017–2019 was measured to be 26.5 μg/m^3 on average (Fig. 5c), which was 1.05, 0.14, and 2.06 times higher than that in O_3- single pollution, $PM_{2.5}$- single pollution, and non-pollution, in respective. These differences in NR-PM_1 among various pollution types were significantly bigger than those in $PM_{2.5}$, in which $PM_{2.5}$ mass concentration in co-pollution was measured to be 60.9 μg/m^3 on average (Fig. 5b), being 1.22, 0.01, and 1.94 times higher than that in O_3- single pollution, $PM_{2.5}$- single pollution, and non-pollution, respectively. As a result of approximately 50% secondary aerosols gathering in NR-PM_1 (Zhang et al., 2019b), it can better reflect the characteristics of secondary conversion than that of $PM_{2.5}$.

Diurnal variations in pollutant concentrations can provide insights into the interplay between emissions and chemical and physical processes that operate on a diurnal cycle (Xu et al., 2021). Thus, to better

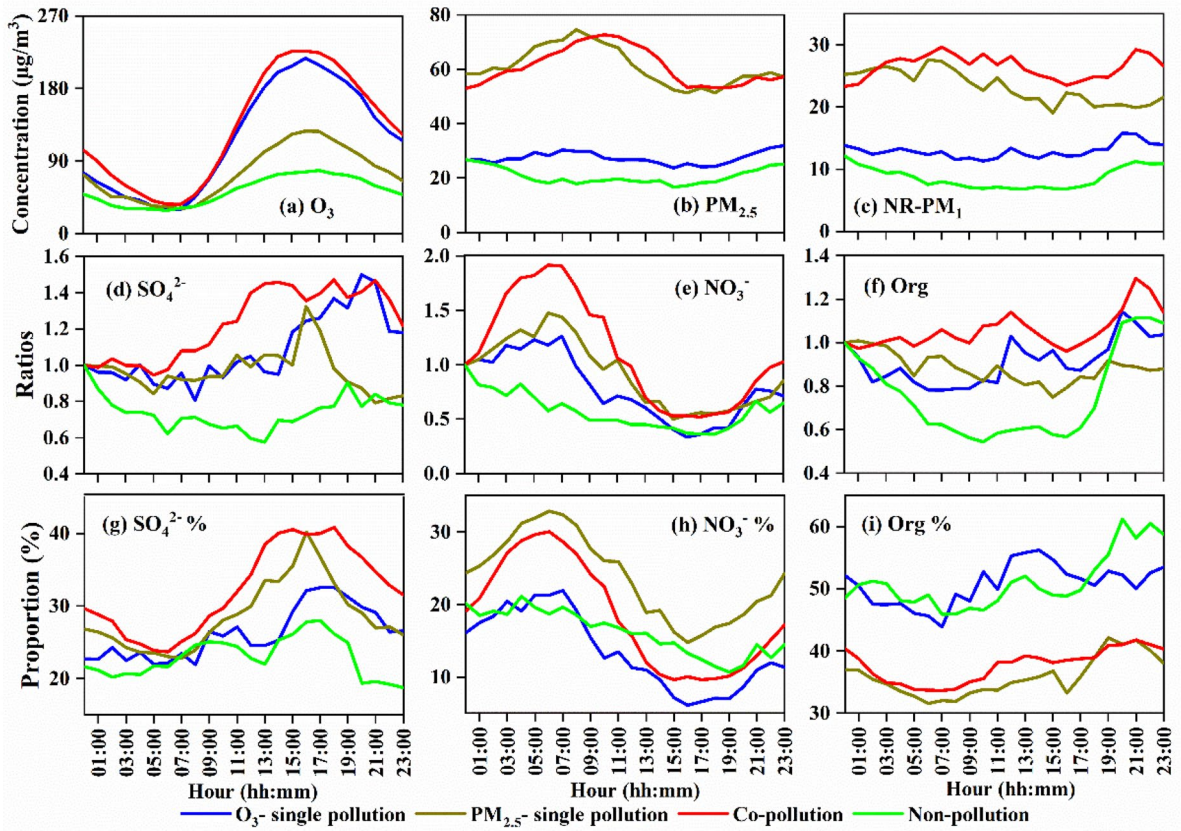

Fig. 5 Diurnal cycles of pollutants in different pollution types during May–September of 2017–2019 in BJ

understand the diurnal changes of various secondary aerosols, their hourly concentrations were normalized to the concentration at 0:00, as shown in Fig. 5d–f. The SO_4^{2-} behaved as a significant contributor in NR-PM_1 in co-pollution, which was consistent with the above-mentioned results of $PM_{2.5}$ (Fig. 4). Its corresponding contribution to NR-PM_1 mass concentration was relatively lower at nighttime (23.7–38.3%), but rapidly rose since the morning and reached the peak in the afternoon (Fig. 5g). This pattern was well consistent with that of O_3 concentrations, illustrating that the augmentation of atmospheric oxidation capacity with high level of O_3 could strengthen the production of secondary particles. The SO_4^{2-} proportion at daytime (8:00–18:00, LT) reached up to 35.5% on average in co-pollution, which was far higher than those in $PM_{2.5}$- single pollution (31.8%) and O_3- single pollution (27.5%), further demonstrating that the important role of SO_4^{2-} in co-pollution. In addition, its proportion at nighttime was comparable to that of co-pollution and O_3- or $PM_{2.5}$-single pollution. These results implied that SO_4^{2-} formation was closely related to daytime photochemistry and gas-phase reactions related to O_3 could be the key channel on the condition of high level of SO_2 and proper RH (Fang et al., 2019; Shon et al., 2012).

However, the behavior of NO_3^- was opposite to that of SO_4^{2-}. The mass proportion of NO_3^- was relatively higher at nighttime than that at daytime. This is because that and the NO_3^- generated by photochemical reactions at daytime could not overcome or counteracted the effects of NO_3^- volatilization induced by the high temperature. Besides, a high level of the NO_3^- at nighttime was associated with the high level of precursor NO_2 on condition of high RH and abundant oxidant (Fig. 3d, m); and heterogeneous hydrolysis of N_2O_5 on humid aerosol surfaces is an important pathway for the formation of NO_3^- at nighttime (Wang et al., 2017). During nighttime, NO_3^- would contribute 21.1% and 25.8% to NR-PM_1 in co-pollution and $PM_{2.5}$-single pollution, respectively, but only 15.8% to NR-PM_1 in O_3-single pollution. This difference might be caused by the fact that the highest level of SO_2 and CO in co-pollution played a key role during this period (Fig. 3j, p).

For Org, its corresponding proportion was relatively higher at daytime (10:00–16:00) in O_3-single pollution but higher at nighttime (19:00–23:00) in $PM_{2.5}$-single pollution. The former reflected the more important role of photochemistry in the formation of secondary organic aerosols, while the latter might indicate the greater impacts of nighttime chemistry, whereas the Org mass concentration in co-pollution were both at a high level at daytime and nighttime. However, the corresponding proportion was lower in co-pollution and $PM_{2.5}$-single pollution than those in O_3-single pollution and non-pollution, indicating that the proportion of carbon components declined with increasing particle concentration. This decrease in the proportions of carbon components from low-level to high-level of particles were similar to other studies in BTH region (Zhao et al., 2019). Overall, the aged or oxidation process of the inorganic was stronger than that of the organic in co-pollution.

Interaction of O_3 and $PM_{2.5}$ in co-pollution

To further explore the interactions between O_3 and $PM_{2.5}$, we analyzed 21 co-pollution episodes occurring in BJ during the study period (Fig. 6a). Among them, 13 episodes were initiated by high level of O_3 mostly occurring about at 13:00, and then the $PM_{2.5}$ concentrations rapidly increased within 2–4 h. This indicated that the augmentation of atmospheric oxidation capacity strengthens the production of secondary particles and thus increased the $PM_{2.5}$ concentrations. The O_3-initiated co-pollution always lasted for approximately 2–7 days. In addition, another 8 episodes were initiated by high level of $PM_{2.5}$ mostly occurring at nighttime (~21:00), leading to the accumulation of precursors, and then the O_3 concentrations slowly increased within 3–6 h. This is mostly because that high level of aerosols causes cooling of the surface, resulting in reduced buoyant turbulence, enhanced atmospheric stratification, and suppressed boundary layer growth (Slater et al., 2020). The $PM_{2.5}$-initiated co-pollution always continued for about 1–3 days, which was evidently shorter than that induced by O_3. This is mostly probably that the co-pollution driven by O_3 was closely related to the chemical processes referred to the augmentation of atmospheric oxidation capacity (Jia et al., 2017), while the co-pollution driven by $PM_{2.5}$ was ascribed to the physical processes involved to unfavorable meteorological conditions. It is worth noting that both the mean MDA8 O_3 and $PM_{2.5}$ concentrations in O_3-initiated co-pollution were significantly

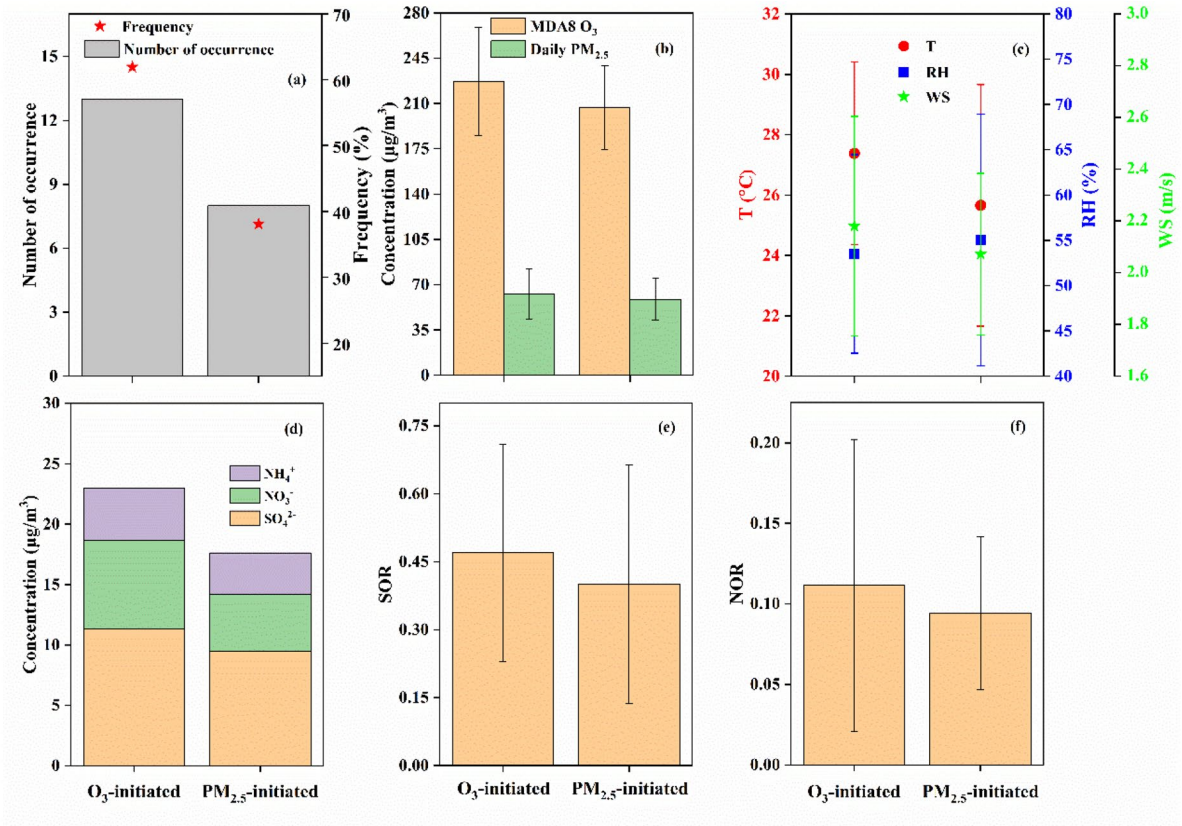

Fig. 6 Characteristics of varied types of co-pollution during May–July of 2017–2019 in BJ

higher than those in $PM_{2.5}$-initiated co-pollution (Fig. 6b), respectively, higher by 20.1 μg/m^3 (10.0%) and 4.2 μg/m^3 (7.1%), highlighting that the enhanced atmospheric oxidation capacity due to high level of O_3 could be the driving force to the formation secondary particles. Moreover, the mean pollution intensity in O_3-initiated co-pollution was slightly higher than that in $PM_{2.5}$-initiated co-pollution, higher by 10.0%.

As expected, a higher T (daily of 27.4 ± 3.0 °C) and lower RH (daily of 53.5 ± 11.0%) as well as lower WS (daily of 2.07 ± 0.31 m/s) were found in O_3-initiated co-pollution (Fig. 6c), in which the higher T would greatly facilitate the occurrence of chemical processes and the lower WS promotes the accumulation of precursors. It is noteworthy that the precursors SO_2 and NO_2 in O_3-initiated co-pollution episodes were slightly higher than those in $PM_{2.5}$-initiated co-pollution episodes, respectively higher by 0.6 μg/m^3 (8.8%) and 1.0 μg/m^3 (2.7%). Such meteorological and chemical conditions were conductive to the formation of secondary particles under the condition of high level of O_3. Combining the concentrations of the inorganic salts in NR-PM_1 and the corresponding gaseous precursors, the sulfur oxidation ratio (SOR) and nitrogen oxidation ratio (NOR) were estimated to evaluate the aging of atmosphere in co-pollution, which was calculated through Eqs. (2) and (3), respectively (Lang et al., 2017; Zhao et al., 2019). Higher values of SOR and NOR reflect greater oxidation of gaseous SO_2 and NO_2, and more secondary aerosols exist in the atmosphere (Huang et al., 2016).

$$\mathrm{SOR} = \frac{n[SO_4^{2-}]}{n[SO_4^{2-}] + n[SO_2]} \quad (2)$$

$$\mathrm{NOR} = \frac{n[NO_3^-]}{n[NO_3^-] + n[NO_2]} \quad (3)$$

where n represents the molar concentration of the corresponding air pollutants (mol/m^3). The SIA concentrations and their proportions in O_3-initated episodes were substantially higher than those in $PM_{2.5}$-initiated episodes, higher by 5.4 μg/m^3 and 6.9%, respectively (Fig. 6d). The mean of daily SOR would reach up to 0.47 ± 0.24 and 0.40 ± 0.26 (Fig. 6e) and that of NOR were 0.11 ± 0.09 and 0.09 ± 0.05 (Fig. 6f) in O_3-initated and $PM_{2.5}$-initiated episodes, respectively. These results indicate that the atmosphere in O_3-initiated episodes was much more aged and oxidized compared with that in $PM_{2.5}$-initiated episodes. This was further approved by the higher "total oxidant" ($O_x = O_3 + NO_2$) production in O_3-initiated episodes, being higher by 4.6% than that in $PM_{2.5}$-initiated episodes.

It can be concluded that (i) in O_3-initiated episodes, the high level of O_3 at daytime induced the raise of $PM_{2.5}$ through facilitating the formation of secondary sulfates on the condition of high level of SO_2, thereby co-pollution occurring, in which chemical processes would be the driving force; (ii) while in $PM_{2.5}$-initiated episodes, high level of $PM_{2.5}$ firstly occurred under the more stable meteorological conditions (high RH and small winds), and then accumulation of gaseous precursors further induced high O_3, in which the physical processes would play a key role.

Conclusions

The monitoring data of O_3 and $PM_{2.5}$ covering all cities of BTH in the hot season during 2015–2019 was analyzed to investigate the variation trends of co-pollution and its causes. It is found that co-pollution of O_3 and $PM_{2.5}$ has become the most predominant type of air pollutions in May–July since 2017 in BTH. And the co-pollution was always accompanied by high T (25.8–28.2 ℃), moderate RH (55.4–63.5%), extremely high SO_2 (5.9–31.1 μg/m^3), and higher NO_2 (36.1–49.8 μg/m^3). MLR analysis showed that O_3 in co-pollution and O_3-single pollution had the comparable dependence on meteorology and precursors, while $PM_{2.5}$ in co-pollution was more sensitive responses to T, RH, and precursors but that in $PM_{2.5}$-single pollution was more sensitive responses to small winds. These results implied that co-pollution seems to be more affected by atmospheric chemistry. Further analysis based on the $PM_{2.5}$ measurements showed that SIA proportion was the highest in co-pollution and accounted for 44.3–48.7% of $PM_{2.5}$ and then $PM_{2.5}$-single pollution (42.1–46.5%) and O_3-single pollution (41.2–44.3%) followed, further highlighting the relatively stronger atmospheric chemistry processes in co-pollution. We found that the extremely high proportion of SIA in co-pollution was mainly attributed to SO_4^{2-}, which was observed to rapidly boom in NR-PM_1 with high level of O_3 at daytime.

Furthermore, the interactions of O_3 and $PM_{2.5}$ in co-pollution were explored based on 21 episodes occurring in Beijing. Most (~61.9%) co-pollution episodes were initiated by high level of O_3 accompanied by high SO_2 at daytime, in which the chemical processes played a key role; as for the rest of the episodes, high $PM_{2.5}$ firstly occurred under the more stable meteorological conditions, and then accumulation of precursors further induced high O_3. The SIA concentration in O_3-initiated co-pollution was higher than that in $PM_{2.5}$-initiated co-pollution, indicating that the atmospheric oxidation in co-pollution caused by chemical processes was stronger than that by physical processes. And it was further approved by the higher values of SOR and NOR in O_3-initiated co-pollution. The key findings revealed that controlling O_3 and precursor SO_2 is the key to abating co-pollution in the hot season. Quantitative study on the control strategies needs to be further carried out by numerical simulation in future.

Acknowledgements The authors are grateful to the anonymous reviewers for their insightful comments.

Author contribution **Shengju Ou**: Investigation, Methodology; Formal analysis, Writing—original draft; **Wei Wei**: Conceptualization; Supervision; Funding acquisition, Writing—Reviewing and Editing; **Bin Cai**: Investigation & Visualization. **Shiyin Yao**: Investigation; **Kai Wang**: Investigation. **Shuiyuan Cheng**: Funding acquisition, Resources.

Funding This work was supported by the National Natural Science Foundation of China (51638001, 52022005) and the Beijing Municipal Commission of Science and Technology (Z181100005418017).

Data availability Hourly pollutant observations, including surface O_3, $PM_{2.5}$, NO_2, SO_2, and CO, can be downloaded from the China National Environmental Monitoring Centre website (CNEMC) (http://www.cnemc.cn/) and archived at https://quotsoft.

net/air/. The surface meteorological parameters, including wind speed, wind direction, temperature, and relative humidity, were obtained from the China Meteorological Administration observation network (http://data.cma.cn/). The data of chemical components that support the findings of this study are available on request from the corresponding author (W. Wei).

Declarations

Competing interest All authors declare no competing interests.

References

Angelevska, B., Atanasova, V., & Andreevski, I. (2021). Urban air quality guidance based on measures categorization in road transport. *Civil Engineering Journal*, *7*(2), 253–267. https://doi.org/10.28991/cej-2021-03091651

Chen, L., Zhu, J., Liao, H., Yang, Y., & Yue, X. (2020). Meteorological influences on $PM_{2.5}$ and O_3 trends and associated health burden since China's clean air actions. *Science of the Total Environment, 744*, 140837. https://doi.org/10.1016/j.scitotenv.2020.140837

Cheng, M., Tang, G., Lv, B., Li, X., Wu, X., Wang, Y., & Wang, Y. (2021). Source apportionment of $PM_{2.5}$ and visibility in Jinan, China. *Journal of Environmental Sciences-China, 102*, 207–215. https://doi.org/10.1016/j.jes.2020.09.012

Fang, Y., Ye, C., Wang, J., Wu, Y., Hu, M., Lin, W., Xu, F., & Zhu, T. (2019). Relative humidity and O_3 concentration as two prerequisites for sulfate formation. *Atmospheric Chemistry and Physics, 19*(19), 12295–12307. https://doi.org/10.5194/acp-19-12295-2019

Fenech, S., Doherty, R. M., Heaviside, C., Macintyre, H. L., O'Connor, F. M., Vardoulakis, S., Neal, L., & Agnew, P. (2019). Meteorological drivers and mortality associated with O_3 and $PM_{2.5}$ air pollution episodes in the UK in 2006. *Atmospheric Environment, 213*, 699–710. https://doi.org/10.1016/j.atmosenv.2019.06.030

Fox, J., & Monette, G. (1992). Generalized collinearity diagnostics. *Journal of American Statistical Association, 87*, 417. https://doi.org/10.1080/01621459.1992.10475190

Gong, C., Liao, H., Zhang, L., Yue, X., Dang, R., & Yang, Y. (2020). Persistent ozone pollution episodes in North China exacerbated by regional transport. *Environmental Pollution, 265*, 115056. https://doi.org/10.1016/j.envpol.2020.115056

Guo, X., Ye, Z., Chen, D., Wu, H., Shen, Y., Liu, J., & Cheng, S. (2020). Prediction and mitigation potential of anthropogenic ammonia emissions within the Beijing-Tianjin-Hebei region, China. *Environmetal Pollution, 259*, 113863. https://doi.org/10.1016/j.envpol.2019.113863

Han, L., Xiang, X., Zhang, H., Cheng, S., Wang, H., Wei, W., Wang, H., & Lang, J. (2019). Insights into submicron particulate evolution, sources and influences on haze pollution in Beijing, China. *Atmospheric Environment, 201*, 360–368. https://doi.org/10.1016/j.atmosenv.2018.12.045

Huang, X., Liu, Z., Zhang, J., Wen, T., Ji, D., & Wang, Y. (2016). Seasonal variation and secondary formation of size-segregated aerosol water-soluble inorganic ions during pollution episodes in Beijing. *Atmospheric Research, 168*, 70–79. https://doi.org/10.1016/j.atmosres.2015.08.021

Hughes, D. D., Christiansen, M. B., Milani, A., Vermeuel, M. P., Novak, G. A., Alwe, H. D., Dickens, A. F., Pierce, R. B., Millet, D. B., Bertram, T. H., Stanier, C. O., & Stone, E. A. (2021). PM2.5 chemistry organosulfates and secondary organic aerosol during the 2017 Lake Michigan Ozone Study. Atmospheric Environment 244, 117939. https://doi.org/10.1016/j.atmosenv.2020.117939

Jia, M., Zhao, T., Cheng, X., et al. (2017). Inverse relations of $PM_{2.5}$ and O_3 in air compound pollution between cold and hot seasons over an urban area of east China. *Atmosphere-Basel, 8*(12), 59. https://doi.org/10.3390/atmos8030059

Kuerban, M., Waili, Y., Fan, F., Liu, Y., Qin, W., Dore, A. J., Peng, J., Xu, W., & Zhang, F. (2020). Spatio-temporal patterns of air pollution in China from 2015 to 2018 and implications for health risks. *Environmental Pollution, 258*, 113659. https://doi.org/10.1016/j.envpol.2019.113659

Lang, J., Zhang, Y., Zhou, Y., et al. (2017). Trends of $PM_{2.5}$ and Chemical Composition in Beijing, 2000–2015. *Aerosol and Air Quality Research, 17*(2), 412–425. https://doi.org/10.4209/aaqr.2016.07.0307

Li, K., Jacob, D. J., Liao, H., Shen, L., Zhang, Q., & Bates, K. H. (2019). Anthropogenic drivers of 2013–2017 trends in summer surface ozone in China. *Proceedings of the National Academy of Sciences, 116*(2), 422–427. https://doi.org/10.1073/pnas.1812168116

Liu, Y., & Wang, T. (2020a). Worsening urban ozone pollution in China from 2013 to 2017-Part 2: The effects of emission changes and implications for multi-pollutant control. *Atmospheric Chemistry and Physics, 20*(11), 6323–6337. https://doi.org/10.5194/acp-20-6323-2020

Liu, Y., & Wang, T. (2020b). Worsening urban ozone pollution in China from 2013 to 2017-Part 1: The complex and varying roles of meteorology. *Atmospheric Chemistry and Physics, 20*(11), 6305–6321. https://doi.org/10.5194/acp-20-6305-2020

Liu, Z., Wang, Y., Hu, B., et al. (2021). Elucidating the quantitative characterization of atmospheric oxidation capacity in Beijing, China. *Science of the Total Environment, 771*, 145306. https://doi.org/10.1016/j.scitotenv.2021.145306

Lu, K., Guo, S., Tan, Z., et al. (2019). Exploring atmospheric free-radical chemistry in China: The self-cleansing capacity and the formation of secondary air pollution. *National Science Review, 6*(3), 579–594. https://doi.org/10.1093/nsr/nwy073

Ma, S., Shao, M., Zhang, Y., Dai, Q., & Xie, M. (2021a). Sensitivity of $PM_{2.5}$ and O_3 pollution episodes to meteorological factors over the North China Plain. *Science of the Total Environment, 792*, 148474. https://doi.org/10.1016/j.scitotenv.2021.148474

Ma, X., Huang, J., Zhao, T., Liu, C., Zhao, K., Xing, J., & Xiao, W. (2021b). Rapid increase in summer surface ozone over the North China Plain during 2013–2019: A side effect of particulate matter reduction control?. *Atmospheric Chemistry and Physics, 21*(1), 1–16. https://doi.org/10.5194/acp-21-1-2021

Porter, W. C., & Heald, C. L. (2019). The mechanisms and meteorological drivers of the summertime ozone-temperature relationship. *Atmospheric Chemistry and Physics, 19*(21), 13367–13381. https://doi.org/10.5194/acp-19-13367-2019

Shao, M., Ren, X., Wang, H., et al. (2004). Quantitative relationship between the generation and elimination of OH and HO_2

radicals in the urban atmosphere. *Chinese Science Bulletin*, *49*(17), 1716–1721. https://kns.cnki.net/kns8/defaultresult/index. 2004-09. (in Chinese). Accessed September 2004.

Shao, M., Wang, W., Yuan, B., et al. (2021). Quantifying the role of $PM_{2.5}$ dropping in variations of ground-level ozone: Inter-comparison between Beijing and Los Angeles. *Science of the Total Environment, 788*, 147712. https://doi.org/10.1016/j.scitotenv.2021.147712

Shon, Z., Kim, K., Song, S., Jung, K., Kim, N., & Lee, J. (2012). Relationship between water-soluble ions in $PM_{2.5}$ and their precursor gases in Seoul megacity. *Atmospheric Environment, 59*, 540–550. https://doi.org/10.1016/j.atmosenv.2012.04.033

Shu, L., Wang, T., Han, H., Xie, M., Chen, P., Li, M., & Wu, H. (2020). Summertime ozone pollution in the Yangtze River Delta of eastern China during 2013–2017: Synoptic impacts and source apportionment. *Environmental Pollution, 257*, 113631. https://doi.org/10.1016/j.envpol.2019.113631

Slater, J., Tonttila, J., McFiggans, G., Connolly, P., Romakkaniemi, S., Kuhn, T., & Coe, H. (2020). Using a coupled large-eddy simulation-aerosol radiation model to investigate urban haze: Sensitivity to aerosol loading and meteorological conditions. *Atmospheric Chemistry and Physics, 20*(20), 11893–11906. https://doi.org/10.5194/acp-20-11893-2020

Wang, G., Cheng, S., Wei, W., Wen, W., Wang, X., & Yao, S. (2015). Chemical characteristics of fine particles emitted from different chinese cooking styles. *Aerosol and Air Quality Research, 15*(6), 2357–2366. https://doi.org/10.4209/aaqr.2015.02.0079

Wang, H., Lu, K., Chen, X., et al. (2017). High N_2O_5 concentrations observed in urban beijing: Implications of a large nitrate formation pathway. *Environmental Science & Technology Letters, 4*(10), 416–420. https://doi.org/10.1021/acs.estlett.7b00341

Wang, Q., Fang, J., Shi, W., & Dong, X. (2020). Distribution characteristics and policy-related improvements of $PM_{2.5}$ and its components in six Chinese cities. *Environmental Pollution, 266*, 115299. https://doi.org/10.1016/j.envpol.2020.115299

Wang, X., Wei, W., Cheng, S., Wang, R., & Zhu, J. (2021). Evaluation of continuous emission reduction effect on PM2.5 pollution improvement through 2013–2018 in Beijing. *Atmospheric Pollution Research, 12*(5), 101055. https://doi.org/10.1016/j.apr.2019.09.004

Xu, J., Huang, X., Wang, N., Li, Y., & Ding, A. (2021). Understanding ozone pollution in the Yangtze River Delta of eastern China from the perspective of diurnal cycles. *Science of the Total Environment, 752*, 141928. https://doi.org/10.1016/j.scitotenv.2020.141928

Xu, W., Kuang, Y., Bian, Y., et al. (2020). Current challenges in visibility improvement in southern china. *Environmental Science & Technology Letters, 7*(6), 395–401. https://doi.org/10.1021/acs.estlett.0c00274

Yang, Y., Ren, L., Li, H., Wang, H., Wang, P., Chen, L., Yue, X., & Liao, H. (2020). Fast climate responses to aerosol emission reductions during the COVID-19 pandemic. *Geophysical Research Letters, 47*, 19. https://doi.org/10.1029/2020GL089788

Yu, Y., Wang, Z., He, T., Meng, X., Xie, S., & Yu, H. (2019). Driving factors of the significant increase in surface ozone in the Yangtze River Delta, China, during 2013–2017. *Atmospheric Pollution Research, 10*(4), 1357–1364. https://doi.org/10.1016/j.apr.2019.03.010

Zha, H., Wang, R., Feng, X., An, C., & Qian, J. (2021). Spatial characteristics of the $PM_{2.5}/PM_{10}$ ratio and its indicative significance regarding air pollution in Hebei Province, China. *Environmental Monitoring and Assessment, 193*, 486. https://doi.org/10.1007/s10661-021-09258-w

Zhang, H., Cheng, S., Li, J., Yao, S., & Wang, X. (2019a). Investigating the aerosol mass and chemical components characteristics and feedback effects on the meteorological factors in the Beijing-Tianjin-Hebei region, China. *Environmental Pollution, 244*, 495–502. https://doi.org/10.1016/j.envpol.2018.10.087

Zhang, H., Cheng, S., Wang, X., Yao, S., & Zhu, F. (2018). Continuous monitoring, compositions analysis and the implication of regional transport for submicron and fine aerosols in Beijing, China. *Atmospheric Environment, 195*, 30–45. https://doi.org/10.1016/j.atmosenv.2018.09.043

Zhang, Q., Jiang, X., Tong, D., et al. (2017). Transboundary health impacts of transported global air pollution and international trade. *Nature, 543*(7647), 705–709. https://doi.org/10.1038/nature21712

Zhang, Q., Quan, J., Tie, X., Li, X., Liu, Q., Gao, Y., & Zhao, D. (2015). Effects of meteorology and secondary particle formation on visibility during heavy haze events in Beijing, China. *Science of the Total Environment, 502*, 578–584. https://doi.org/10.1016/j.scitotenv.2014.09.079

Zhang, Q., Zheng, Y., Tong, D., et al. (2019b). Drivers of improved PM2.5 air quality in China from 2013 to 2017. *Proceedings of the National Academy of Sciences, 116*(49), 24463–24469. https://doi.org/10.1073/pnas.1907956116

Zhao, D., Liu, G., Xin, J., et al. (2020). Haze pollution under a high atmospheric oxidization capacity in summer in Beijing: Insights into formation mechanism of atmospheric physicochemical processes. *Atmospheric Chemistry and Physics, 20*(8), 4575–4592. https://doi.org/10.5194/acp-20-4575-2020

Zhao, L., Wang, L., Tan, J., et al. (2019). Changes of chemical composition and source apportionment of PM2.5 during 2013–2017 in urban Handan, China. *Atmospheric Environment, 206*, 119–131. https://doi.org/10.1016/j.atmosenv.2019.02.034